Transport properties of separated pairs of CuO_2 planes in $(Pb_2Cu)Sr_2Dy_xCe_{n-x-\delta}Cu_2O_{2n+6}$ $(n=3,5)$ epitaxial films

Sumio Ikegawa and Yuichi Motoi
Advanced Materials & Devices Laboratory, Corporate Research & Development Center, Toshiba Corporation, 1, Komukai Toshiba-cho, Saiwai-ku, Kawasaki 212-8582, Japan
(Received 27 August 1999)

The in-plane resistivity and thermopower for Pb-32n2 phase, $(Pb_2Cu)Sr_2Ln_xCe_{n-x-\delta}Cu_2O_{2n+6}$ (Ln=Dy or Eu, $n=3$ or 5), have been studied. The distance, d, between a pair of CuO_2 planes can be arbitrarily chosen in the Pb-32n2 family. So, one can expect the control of electronic anisotropy using this family. The samples were grown by sequential deposition using the molecular beam epitaxy technique. The hole concentration per [CuO], p, was estimated from the thermopower at room temperature. The highest value of p for the Pb-3252 film sample is 0.089, which is within the range for the occurrence of superconductivity in layered cuprates, although resistivity of the Pb-3252 sample shows weak localization behavior. The increase in hole concentration by the substitution of Dy^{3+} for Ce^{4+} is lower than expected from the simple calculation of the valence. We discuss possible reasons for these findings and for the absence of superconductivity. The cation deficiency in the fluorite block is supposed to be one of the reasons for the low efficiency of carrier doping and localization behavior. Sheet conductance per CuO_2 plane is similar for the Pb-3232 phase ($d=0.87$ nm) and Pb-3252 phase ($d=1.41$ nm).

I. INTRODUCTION

It is widely recognized that the high-T_c superconductors consist of a natural arrangement of stacked Josephson junctions, which are called intrinsic Josephson junctions, because of their layered crystal structure. The intrinsic junctions have high performance, such as high I_cR_N product and SIS tunnel type characteristics.[1] They are free from the problems of reducing the I_cR_N product[2] caused by misorientation between two d-wave superconductors. However, the series array of the same junctions alone is not very useful for electronic applications: technologies for making thick superconducting electrodes beside the junctions or for making a single junction at any place are needed. Thus, the control of Josephson coupling in the arbitrary unit cell of stacked layered cuprates is desirable in electronic applications.

In a layered cuprate having a multiple fluorite-type block, $(Pb_2Cu)Sr_2(Ln,Ce)_nCu_2O_{6+2n-z}$ ($n\geqslant 2$, Ln=rare earth element) (Pb-32n2 phase), the distance between a pair of CuO_2 planes can be arbitrarily chosen. So, the Pb-32n2 family offers the potential to control electronic anisotropy or the strength of Josephson coupling along the c-axis.[3,4] The crystal structure of the Pb-3252 phase is shown in Fig. 1. This family is a unique system in that the distance, d, between the bases of a pair of pyramidal Cu-O planes across the fluorite-type block can be changed with a unit thickness of 0.27 nm through changing the layer number, n, of the rare-earth oxide. In the CuO_2 plane, Cu and O atoms are not located on exactly the same plane. If the position of the CuO_2 plane is approximated by the center of the Cu plane and O_2 plane, d is expressed as $d=0.6+0.27(n-2)$ nm.

Apart from the applications, the effect of interlayer coupling is a key issue.[5] There are theoretical studies which describe the interlayer pair tunneling energy as the main contribution to the condensation energy of high-T_c superconductor.[6,7] This is called an interlayer tunneling mechanism. There is also the theory that interlayer Cooper pair formation contributes to superconductivity.[8,9] In fact, the pair of CuO_2 planes in which an atomic plane consisting of a rare earth element or calcium is inserted ($d=0.31$ nm), often exhibits superconductivity at temperatures above the temperature of liquid nitrogen. Thus, it is important to know how transport properties are affected by changing the distance d, for the understanding of high-temperature superconductivity. So far, many superconductors having a fluorite-type block with $n=2$, such as T^* phase[10] and Bi-2222 phase,[11] have been reported. However, it is difficult for the layered cuprates having a multiple fluorite-type block with $n\geqslant 3$ to exhibit superconductivity[12,13,14,15] with one exception.[16] The reason for this needs to be clarified.

Recently, epitaxial films of Pb-32n2 with $n=3-8$ have

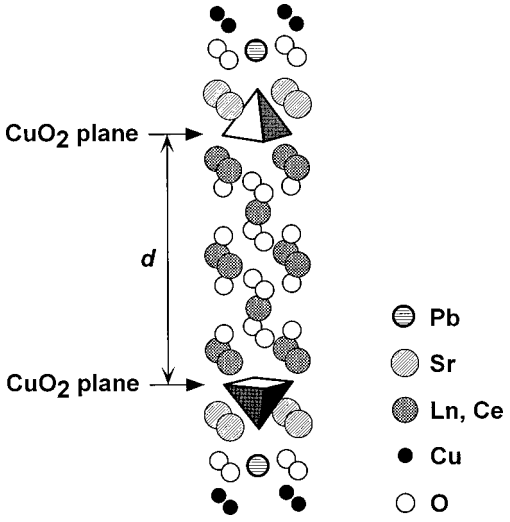

FIG. 1. Crystal structure of Pb-3252 phase.

been successfully grown by the molecular beam epitaxy (MBE) technique.[3] A well-controlled thin-film process including sequential deposition enabled us to obtain a single phase with $n>4$, which is difficult to achieve by the bulk method.[14,15] We have proposed such a structure for high-performance trilayer Josephson junctions: a layer of Pb-32n2 one unit cell thick with $n=3-8$ sandwiched between two Pb-3212 superconducting electrodes.[3] The multiple fluorite-type block, $[(Ln,Ce)O_2]_n$, in the Pb-32n2 phase is probably an insulator and is in direct contact with the CuO_2 plane. If the superconducting order parameter extends to this CuO_2 plane, it seems to be an ideal atomic arrangement at the superconductor-insulator interface. To achieve this, the CuO_2 planes in the Pb-32n2 phase should be doped with carriers with the same level as the superconductor: i.e., $0.05<p<0.3$.

Until now, little has been known about the transport properties of the Pb-32n2 phase with $n>3$. In this paper, we report the in-plane transport properties of Pb-32n2 films with $n=3$ and 5, and compare them with those of Pb-3212 films. The primary purpose of the work reported in this paper is to understand how the carriers are doped by cation substitution. The secondary purpose is to address the problems of why it is difficult for the Pb-32n2 phase with $n\geqslant 3$ to exhibit superconductivity, and how transport properties are affected by changing the distance d.

II. EXPERIMENTS

The c-axis oriented films with nominal compositions of $(Pb_2Cu)Sr_2Dy_{1-y}Ca_yCu_2O_{8+z}$ (Pb-3212 phase), $(Pb_2Cu)Sr_2Dy_xCe_{3-x-\delta}Cu_2O_{12-z}$ (Pb-3232 phase), and $(Pb_2Cu)Sr_2Ln_xCe_{5-x-\delta}Cu_2O_{16-z}$ (Ln=Dy, Eu) (Pb-3252 phase) were grown by the molecular beam epitaxy (MBE) technique. The MBE growth of the Pb-3212 phase was previously reported.[17] Pb, Sr, Ca, Dy or Eu, Ce, and Cu metals were evaporated from the effusion cells onto a $SrTiO_3$ (001) surface. The growth temperature was 873–1073 K, which was measured by using an optical pyrometer. The probing wavelength of the pyrometer ranged from 8 μm to 13 μm. The flux density from each metal source was adjusted individually prior to growth. The fluxes of each metal were supplied sequentially to the substrate in accordance with the stacking order of elements in the Pb-32n2 crystal structure. The shuttering sequence was repeated 25–30 times, corresponding to the film thickness of 39.5–80.7 nm. For the growth of the Pb-3232 and Pb-3252 films, an undercoat consisting of two- or three-unit-cell-thick Pb-3212 phase was deposited on the substrate surface. The composition of the undercoat was chosen to give low carrier concentration and high resistivity. Resistivity and thermopower for the undercoat alone were measured. The contribution of the undercoat to the measured data in Figs. 8 and 9 was estimated to be less than 0.1% of the resistivity and less than 1% of the thermopower. Gaseous oxygen activated by an ECR plasma or pure ozone gas[18] was continuously supplied to the substrate during growth. The typical ozone pressure during growth was 2×10^{-4} Pa.

The growth mechanisms have been investigated by *in situ* reflection high-energy electron diffraction (RHEED). A 25 kV electron beam was used with an incident angle of 2°.

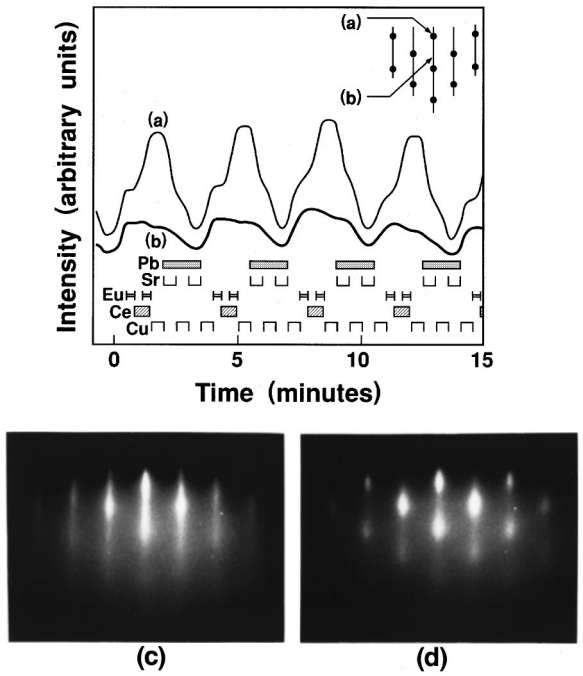

FIG. 2. RHEED observation during growth of Pb-3242 phase. (a) Intensity of the spot as a function of time; (b) intensity of the streak as a function of time. The bars below the curves indicate the interval during which each shutter was open. (c) RHEED pattern after deposition of CuO_2 plane and before deposition of fluorite block; (d) RHEED pattern during the growth of fluorite block.

RHEED patterns were observed along the [100] azimuth of the substrate. The characteristic growth mechanism of the Pb-32n2 phase ($n=3-8$) is the self-organized formation of the layered structure.[3] Figures 2(a) and 2(b) show typical oscillation of RHEED intensity during growth of the Pb-32n2 phase ($n=3-8$). During the deposition of the fluorite block $[(Ln,Ce)O_2]_n$, the spot pattern is superposed on the streak pattern as shown in Fig. 2(d), and the intensity of the spot [Fig. 2(a)] increases. This spot pattern is similar to the case of island growth of (100)-oriented CeO_2 film with {111} facets. The island structure may be stabilized by exposure of the thermodynamically stable surface of the fluorite structure. However, during deposition of Pb oxide, the intensity of the spot decreases. After deposition of the next CuO_2 plane, the streak pattern is restored to its original shape, as shown in Fig. 2(c). This suggests that the reactions and formation of the one-unit-cell-thick Pb-32n2 phase recover the surface flatness from the rugged surface of the fluorite-type oxide. We have synthesized superlattices of alternating one-unit-cell-thick (3.23 nm) layers of Pb-3272 with two-unit-cell-thick layers of Pb-3212. The x-ray diffraction pattern of this superlattice was previously reported and agreed well with the calculated pattern.[3] Figure 3 shows the cross-sectional transmission electron microscopy (TEM) image of this superlattice. It shows regularly aligned dark bands, which are fluorite blocks. Heavy ions, Eu and Ce, make the fluorite blocks dark. The flat fluorite blocks in this figure suggest that the formation of the Pb-32n2 layered compound overcomes the island growth of the fluorite-type oxide.

After the film growth, the phases present and lattice constants were determined by x-ray diffraction (XRD), using

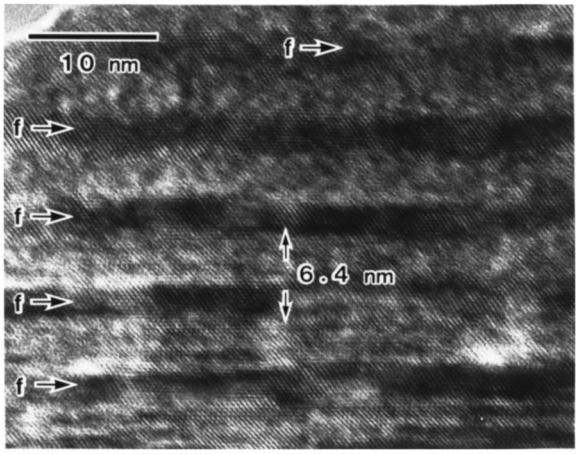

FIG. 3. Cross-sectional TEM image of $[\text{Pb-3272}/(\text{Pb-3212})_2]_{15}$ superlattice. The period of the superlattice (6.4 nm) is clearly visible. The fluorite block is labeled ''*f*.''

Cu-$K\alpha$ radiation. The chemical composition of the films was analyzed by inductively coupled plasma (ICP) emission spectroscopy and was expressed as the number of atoms per *ab*-plane unit cell area (0.148 nm^2) per shuttering cycle. The total accuracy of the ICP measurements was estimated to be within 2%. The compositions and the *c*-axis lattice parameter of the Pb-3252 and Pb-3232 samples for transport measurements are given in Table I. It should be noted that the Sr compositions in the Pb-3252 and Pb-3232 samples were not directly measured, but estimated from the flux monitor, since the dissolve procedure for these films also dissolves the $SrTiO_3$ substrate. For transport measurements, silver was evaporated onto the film for contacts. Resistivity measurements were carried out by a conventional dc four-probe method in the temperature range between 2 and 300 K. Thermoelectric power was measured by a steady-state technique at temperatures between 40 and 300 K. The temperature and temperature gradient across the sample were measured using a calibrated Pt sensor and two pairs of Cu-Constantan thermocouples, respectively. Cu wires of 50-μm diameter were used as the reference metal.

It is well known that the hole concentration, *p*, per $[\text{CuO}]^{+p}$ is the most important parameter, determining both the normal-state and superconducting-state properties of layered cuprates. Tallon *et al.*[19] found a universal relation between the thermopower at room temperature, S_{290}, and *p*, for various layered cuprates. Thus, S_{290} is thought to be a measure of *p* in all the layered cuprates. We used the following equations derived from Tallon's universal curve to evaluate the hole concentration of the film samples:

$$p = -\frac{1}{32.4}\ln\left(\frac{S_{290}}{372}\right) \quad \text{for } 0 < p \leqslant 0.04,$$

$$p = -\frac{1}{25.3}\ln\left(\frac{S_{290}}{278}\right) \quad \text{for } 0.04 < p \leqslant 0.10,$$

$$p = -\frac{1}{38.1}\ln\left(\frac{S_{290}}{992}\right) \quad \text{for } 0.10 < p \leqslant 0.155.$$

TABLE I. Phase, Dy content (x), composition, cation deficiency in the fluorite block (δ), and *c*-axis lattice parameter (c) of the film samples for transport measurements.

Phase	x	Composition	δ	c (nm)
Pb-3252	0.97	$Pb_{1.20}Sr_{2.2}Dy_{0.97}Ce_{3.16}Cu_{2.92}O_y$	0.87	2.683
Pb-3252	1.48	$Pb_{1.38}Sr_{2.2}Dy_{1.48}Ce_{2.74}Cu_{2.95}O_y$	0.78	2.688
Pb-3252	1.86	$Pb_{1.60}Sr_{2.3}Dy_{1.86}Ce_{2.79}Cu_{2.88}O_y$	0.35	2.688
Pb-3232	0.84	$Pb_{1.88}Sr_{2.1}Dy_{0.84}Ce_{1.50}Cu_{2.83}O_y$	0.66	2.139
Pb-3232	1.00	$Pb_{2.14}Sr_{2.1}Dy_{1.00}Ce_{1.36}Cu_{3.06}O_y$	0.64	2.139
Pb-3232	1.44	$Pb_{2.20}Sr_{2.1}Dy_{1.44}Ce_{0.93}Cu_{3.02}O_y$	0.63	2.138

This is a valuable method for evaluating the *p* value of layered cuprate thin films, since an analysis of oxygen content, an iodometric titration technique, and a Coulometric titration technique, which are used for determining the *p* value in bulk samples, are not applicable to thin-film samples.

III. RESULTS

A. Structural chemistry

First, we deal with the structural chemistry of the film samples. RHEED observations show that the Pb-32*n*2 phase with $n=1$, 3, and 5 were epitaxially grown on the substrate in two-dimensional growth mode with the growth unit of a unit cell. Figure 4 shows XRD patterns for Pb-3252 and Pb-3232 films. Open squares indicate the peaks due to the substrate and closed circles indicate the peaks due to the undercoat. There are no peaks due to impurity phases. An XRD pattern assuming the ideal crystal structure was calculated taking into account the Laue function, the structure factor, the Lorentz factor for a single-crystal film, and the absorption factor for a finite-thickness film, as shown in Figs. 4(b) and 4(d). We referred to Cava *et al.*[20] for the crystal structure of the Pb-3212 phase, and to Wada *et al.*[13] for the atom positions of the double fluorite block, $[(\text{Ln, Ce})\text{O}_2]_3$. The atom positions of the Pb-3252 phase were extrapolated by assuming that the CeO_2 layers were inserted in the center of the double fluorite block (see Fig. 1). The relative intensities of measured XRD patterns [Figs. 4(a) and 4(c)] qualitatively agreed with those of the calculated ones [Figs. 4(b) and 4(d)]. Thus, the desired crystal structures were obtained although some cation vacancies were present (see Table I). All the samples in Figs. 7–11 were confirmed by XRD to be of single phase.

Depending on the rare earth content, a Pb-32*n*2 phase with different *n* value is obtained.[3] The *c*-axis length, obtained from the XRD pattern, was investigated as a function of the rare earth compositions. The results are shown in Fig. 5. The horizontal axis indicates the composition of rare earth elements, *w*, in a unit cell of $(\text{Pb}_2\text{Cu})\text{Sr}_2(\text{Ln, Ce})_w\text{Cu}_2\text{O}_v$ (Ln=Eu, Dy), measured by ICP analysis. The ideal value of *w* should be 5.0 for the Pb-3252 phase. The Pb-3252 films, however, were grown for $w=3.8-4.7$. On the other hand, the Pb-3262 film was grown for $w=5.0$. This suggests that cation deficiency, δ, exists in the fluorite block of the Pb-3252 phase. For the Pb-3232 phase, the cation deficiency in the fluorite block is also evident. The values of δ for the transport measurement samples are shown in Table I.

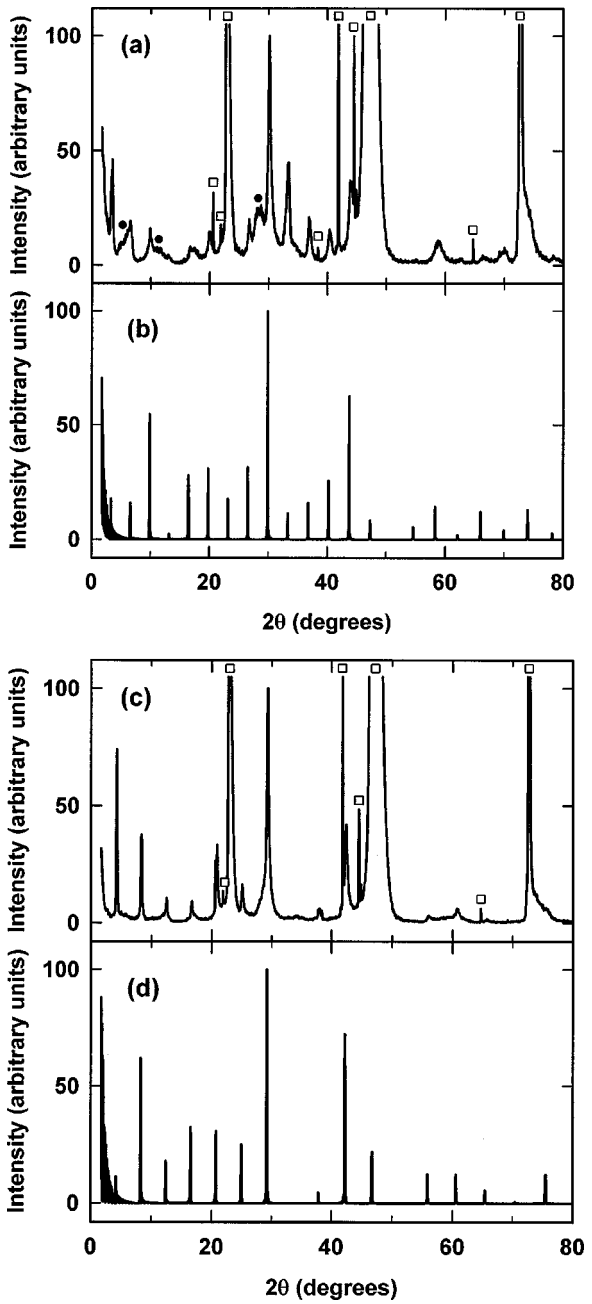

FIG. 4. X-ray diffraction patterns. (a) Experimental result for the Pb-3252 film; (b) calculated diffraction pattern for the Pb-3252 film; (c) experimental result for the Pb-3232 film; (d) calculated diffraction pattern for the Pb-3232 film. Open squares indicate the peaks due to the substrate and closed circles indicate the peaks due to the undercoat.

B. Dependence on growth temperature

Before investigating the transport properties of the thin-film materials, various growth conditions should be optimized. We previously reported the optimization of oxygenation conditions during growth and during the cooling process after growth.[4] In general, the quality of crystal and electric conductivity of the cuprate films strongly depends on the growth temperature. So, we made Pb-3252 phase films [nominal compositions: $(Pb_2Cu)Sr_2Eu_xCe_{5-x-\delta}Cu_2O_{16-z}$ ($x=1.4$)] at various growth temperatures, T_{gr}. Resistivity of the samples is shown in Fig. 6 as a function of $T^{-1/3}$. The

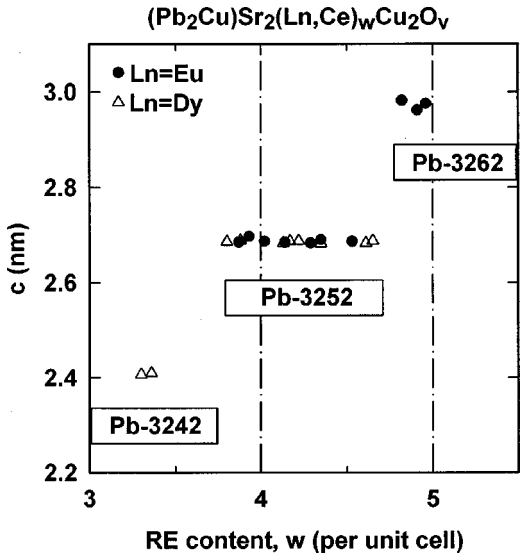

FIG. 5. Lattice constant, c, vs the rare earth composition in a unit cell, w.

oxygenation condition during growth was optimized for each growth temperature. The samples with $T_{gr}<1003\,\mathrm{K}$ were found to be a single phase of the Pb-3252 phase, whereas the samples with $T_{gr}\geqslant 1003\,\mathrm{K}$ included Pb-3212 phase and CeO_2 as impurity phases. The lowest resistivity was obtained in the case of $T_{gr}=973\,\mathrm{K}$. In the following experiments, the growth temperature was 973 K.

In Fig. 6, the temperature dependences of the logarithm of resistivity can be classified into two categories. Low-resistivity samples, such as for $T_{gr}=953$ and 973 K, show $\rho\propto\exp(T^{-1/3})$ at $T<100\,\mathrm{K}$, as is evidenced by the straight line in Fig. 6. This may be attributed to two-dimensional variable range hopping (VRH) transport. The two-dimensional (2D) characteristics in transport are expected in the Pb-3252 phase, since the CuO_2 plane in this compound is rather isolated. The distance between the CuO_2 planes is 1.41 nm across the fluorite block layer, and is 1.27 nm across the

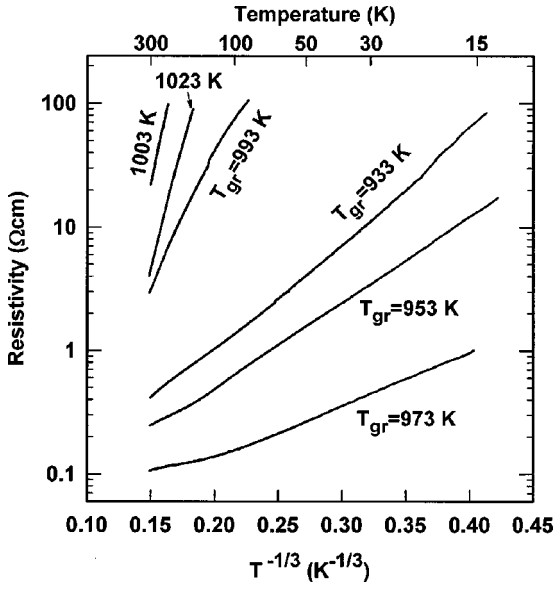

FIG. 6. Resistivity vs $T^{-1/3}$ for Pb-3252 films. The curves are labeled according to the growth temperature.

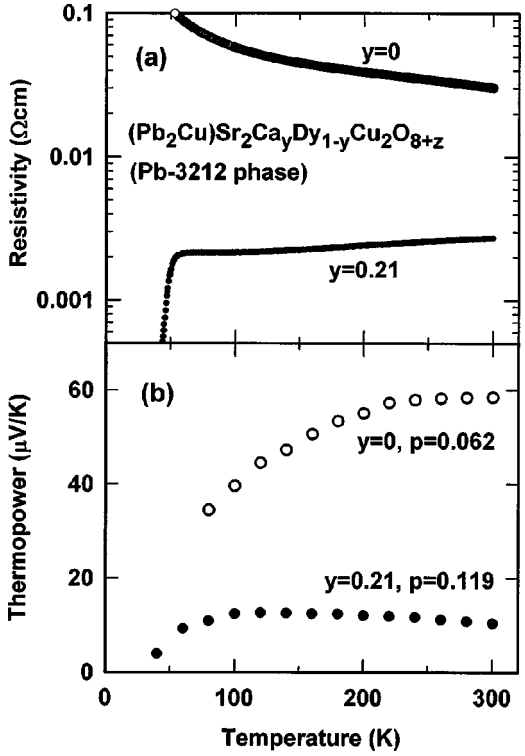

FIG. 7. Temperature dependence of (a) resistivity and (b) thermopower for Pb-3212 films. The film compositions are $Pb_{1.00}Sr_{2.40}Dy_{1.19}Cu_{2.82}O_{\nu}$ $(y=0)$ and $Pb_{0.99}Sr_{2.24}Dy_{0.77}Ca_{0.21}Cu_{2.93}O_{\nu}$ $(y=0.21)$.

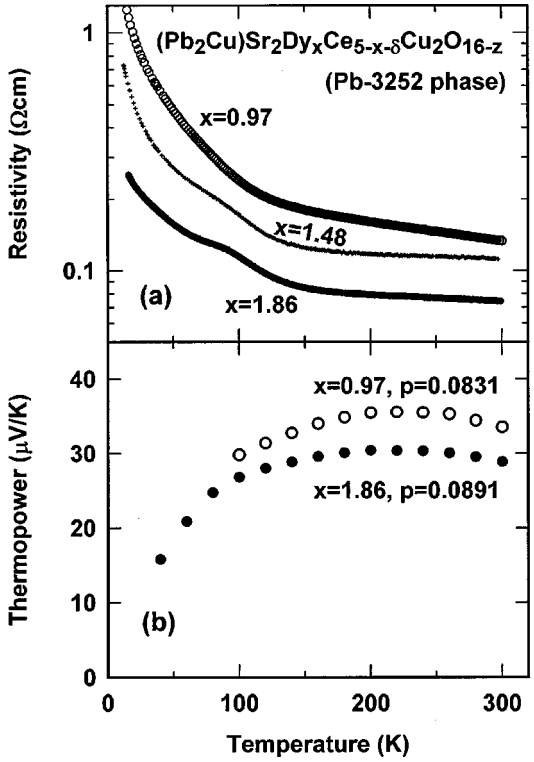

FIG. 8. Temperature dependence of (a) resistivity and (b) thermopower for Pb-3252 films.

[SrO-PbO-Cu-PbO-SrO] block layer. On the other hand, high-resistivity samples such as for $T_{gr}=993$, 1003, and 1023 K show $\rho \propto \exp(T^{-1/4})$, as is seen by the negative curvature in Fig. 6. This may be attributed to three-dimensional VRH. In the high resistivity samples, the strength of disorder in the CuO_2 planes may be so high that the expected two-dimensional transport is hindered. As will be shown later in Sec. III D the resistivity of the Pb-3252 film is found to be lower as a result of further studies. In this case, the temperature dependence of resistivity becomes weaker than $\exp(T^{-1/4})$ and $\exp(T^{-1/3})$, suggesting a weak localization.

C. Transport properties of Pb-3212 films

Transport properties for Pb-3212 phase films [nominal compositions: $(Pb_2Cu)Sr_2Dy_{1-y}Ca_yCu_2O_8$] were investigated as a reference for Pb32n2 $(n=3,5)$ films. The hole concentration, p, would increase with Ca content following the relation $p=y/2$, from the simple calculation of the valence, assuming that the substitution does not create compensating defects. Figure 7 shows the logarithm of resistivity and thermopower as a function of temperature. Resistivity and thermopower decrease with Ca doping. The thermopower data in Fig. 7(b) are consistent with the reported data for $(Pb_2Cu)Sr_2Y_{1-y}Ca_yCu_2O_8$ single crystals.[21] The values of p for each sample were estimated to be 0.062 for $y=0$ and 0.119 for $y=0.21$. These values agree well with the expectation from the simple calculation of the valence.

The Ca doping with $y=0.21$ brought a transition from insulator to superconductor. The superconducting transition temperature for $y=0.21$ was determined from resistive transition. The temperatures where resistivity drops to 50% and 10% of the normal-state resistivity are 47.2 K and 41.6 K, respectively. These values are similar to the reported values for bulk ceramics of $(Pb_2Cu)Sr_2Y_{1-y}Ca_yCu_2O_{8+z}$ with $y=0.15-0.2$.[22]

D. Transport properties of Pb-3252 films

The cation substitution of Ce^{4+} by Dy^{3+} to change the carrier density in Pb-3252 phase films [nominal compositions: $(Pb_2Cu)Sr_2Dy_xCe_{5-x-\delta}Cu_2O_{16-z}$] was studied. From the simple calculation of the valence assuming $z=0$ and $\delta=0$, p would increase with Dy concentration, x, following the relation $p=(1-x)/2$. The temperature dependences of the logarithm of the in-plane resistivity and in-plane thermopower are shown in Figs. 8(a) and 8(b), respectively. Resistivity and thermopower decrease with Dy content. The most conductive sample has a resistivity of $7.43\times10^{-2}\,\Omega$ cm at $T=298$ K, and $1.75\times10^{-1}\,\Omega$ cm at $T=40$ K. The conductivity of the Pb-3252 sample has been improved by a factor of 26 at $T=298$ K, and 430 at $T=40$ K, as compared with the previous report.[4] This improvement was achieved after the optimization of film compositions and growth conditions, such as growth temperature, and oxygenation conditions during the growth and during the cooling process after growth.

The temperature dependence of resistivity for the most conductive sample in Fig. 8(a) is weaker than $\exp(T^{-1/4})$ and $\exp(T^{-1/3})$. This temperature dependence is no longer explained by VRH, in contrast to the data in Fig. 6. The resistivity is proportional to $\ln T$ at temperatures below 60 K. This may be due to the weak localization effect and/or effects of Coulomb interaction between electrons in a random potential

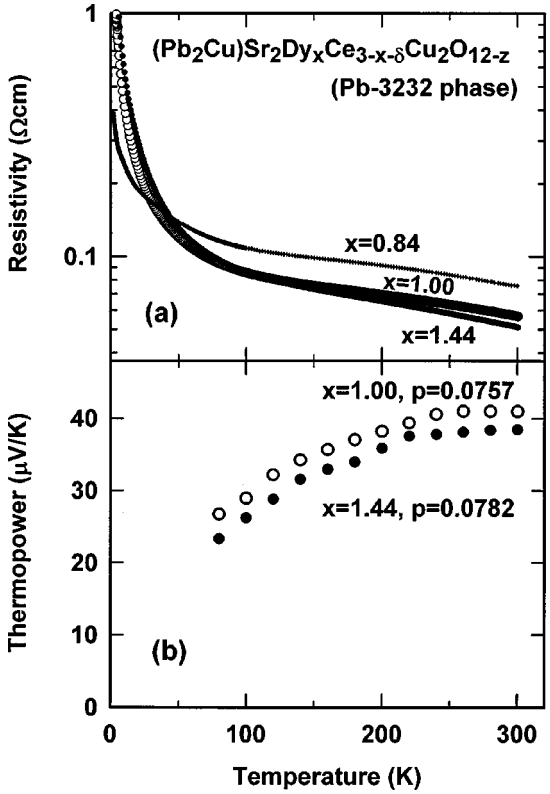

FIG. 9. Temperature dependence of (a) resistivity and (b) thermopower for Pb-3232 films.

in the two-dimensional system. Theoretically, the localization and interaction corrections to sheet conductance of 2D disordered electronic systems are expressed as $\sigma(T)=\sigma_0+(\alpha e^2/2\pi^2\hbar)\ln(T/T_0)$, where α is an order of unity.[23] The plot of sheet conductance of our film vs $\ln T$ appears to be linear at temperatures below 40 K, and α is estimated to be 1.2 in this temperature region. The value of α is consistent with the theory.

The hole densities were estimated from the room-temperature thermopower. A slight increase in p with x was observed from $p=0.0831$ for $x=0.97$ to $p=0.0891$ for $x=1.86$. The substitution of Ce^{4+} by Dy^{3+} increased the hole density, but the densities obtained disagreed with the expectation from the simple calculation of the valence, regarding the following two points. First, a self-doping of holes was observed in the sample with $x=0.97$ where we intended to make the parent compound before hole doping. Second, the hole concentration for the sample with $x=1.86$ was smaller than expected. This means that the efficiency of hole doping with cation substitution is very low.

A generic phase diagram for the superconducting cuprates shows that superconductivity occurs when $0.05<p<0.3$. The largest value of p in our Pb-3252 samples was 0.0891. This is in the range of superconductivity. However, the resistivity showed not metallic but weak localization behavior. This is in good contrast to the Pb-3212 phase, where the insulator-superconductor transition occurs with the cation substitution of 0.21.

E. Transport properties of Pb-3232 films

Transport properties of the Pb-3232 phase [nominal compositions: $(Pb_2Cu)Sr_2Dy_xCe_{3-x-\delta}Cu_2O_{12-z}$] were studied as a function of the Dy content. The distance between CuO_2 planes across the fluorite block in the Pb-3232 phase is between those of Pb-3212 and Pb-3252, and is 0.87 nm. The growth conditions were the same as those for Pb-3252 in Fig. 8. As in the case of Pb-3252, the substitution of the Ce^{4+} ion by Dy^{3+} in the Pb-3232 phase was expected to increase the carrier density following the relation $p=(1-x)/2$, if the substitution did not create compensating defects such as oxygen vacancies. Resistivity [Fig. 9(a)] at temperatures higher than 100 K and thermopower [Fig. 9(b)] decreased with Dy content.

The values of p estimated from room-temperature thermopower were 0.0757 for $x=1.00$ and 0.0782 for $x=1.44$. Similar to the Pb-3252 phase, a self-doping of holes was observed in the Pb-3232 sample with $x=1.00$, where we intended to make the parent compound before hole doping, and the efficiency of hole doping with cation substitution was very low.

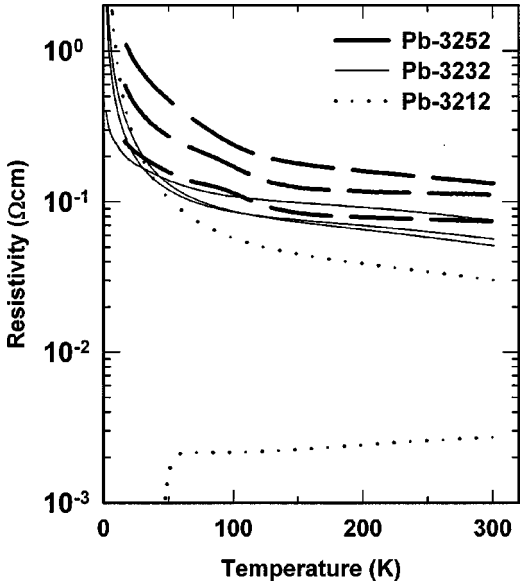

FIG. 10. Comparison of resistivity for Pb-32n2 phase with $n=1$, 3, 5.

F. Comparison of Pb-32n2 ($n=1,3,5$)

The resistivity of the Pb-32n2 phase with $n=1$, 3, and 5 is compared in Fig. 10. Two or three samples with different doping levels for each phase are shown: all the data were taken from Figs. 7, 8, and 9. The resistivity appears to increase with n. To investigate conducting properties of each CuO_2 plane, the data in Fig. 10 were converted to the sheet resistance per CuO_2 plane, as shown in Fig. 11. The best conducting sample in the Pb-3252 phase has a sheet resistance value similar to the best conducting sample in the Pb-3232 phase. This suggests that the electric conduction within a CuO_2 plane does not deteriorate with the increase of d from 0.87 nm ($n=3$) to 1.41 nm ($n=5$). Resistivity of the Pb-3252 phase is greater than that of the Pb-3232 phase merely because the number of conduction planes per unit volume is smaller in the former. It should be noted that the sheet resistance per CuO_2 plane of carrier doped Pb-3252 and Pb-3232 samples is nearly the same as that of the nondoped Pb-3212 phase.

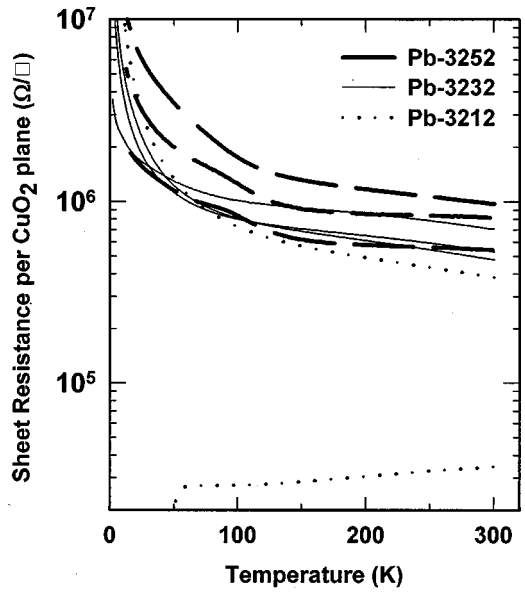

FIG. 11. Sheet resistance per CuO_2 plane for Pb-32n2 phase with $n=1$, 3, 5.

IV. DISCUSSION

The carrier doping characteristics of Pb-3232 and Pb-3252 phases are summarized as follows. First, self-doping of holes was observed in the sample where we intended to make the parent compound before hole-doping. Second, a gain in the hole concentration by the cation substitution in the fluorite block was smaller than expected. We mentioned in Sec. III A that cation deficiency existed in the fluorite type block layer. The cation deficiency may cause the self-doping. One of the reasons for the second characteristic is that the substitution of the Ce^{4+} ion by Dy^{3+} creates compensating oxygen vacancies. The cation deficiency in the fluorite block may promote creation of such oxygen vacancies.

The mechanism by which the cation deficiency is created is probably related to the growth mechanism of the Pb-32n2 phase mentioned in Sec. II. During the growth of the fluorite block, island growth with facets occurred. The following self-organized formation of the layered structure made the flat fluorite block layer. The cation vacancies may be left in the fluorite block during this flattening process.

Next, we discuss why superconductivity is hard to obtain in layered cuprates having a multiple fluorite-type block layer. According to the interlayer tunneling model,[6,7] T_c would decrease with increasing d, because the absolute value of the Josephson coupling energy and consequently the condensation energy of the superconductor decrease. The theory considering the interlayer Cooper pair formation[8] suggests that T_c decreases with increasing d, as a consequence of the decrease in the coupling constant of interlayer pairing interaction. Both of the models predict that the values of T_c for the Pb-3232 and Pb-3252 phase are lower than that for the Pb-3212 phase. The present study showed that the Pb-32n2 compound with $n=3$ and 5 did not exhibit superconductivity down to 2 K, in spite of the fact that the hole density was sufficient for superconductivity, although the density was somewhat lower than the optimal value ($p=0.15-0.2$). It should be noted that resistivity of the Pb-3232 and Pb-3252 sample increases with decreasing temperature. We have to consider why metallic conduction is not obtained, before discussing the comparison of the above-mentioned models with the experimental results.

The resistivity of Pb-3252 phase suggests the weak localization and/or effects of the interaction between electrons in the disordered two-dimensional electronic system (see Sec. III D). Then, it is supposed that a disordered potential yielded in the CuO_2 planes destroys the superconductivity. In the Pb-3252 phase, the dimensionality of electronic system is expected to be lower than that of Pb-3212. If the dimensionality becomes lower from three to two, the wave function of charge carrier tends to be more strongly localized and electric conduction is influenced more strongly by the disordered potential.[23] One of the possible sources of the disordered potential for charge carriers is the cation deficiency in the fluorite-type block layer. This is considered to be one of the reasons for the absence of superconductivity in the Pb-32n2 phase with $n\geqslant 3$. Note that the occurrence of superconductivity in $(Ln_{2/3}Ce_{1/3})_2(La_{1/3}Ba_{1/3}Sr_{1/3})_2Cu_3O_{9-z}$ depends on the ionic radius of the rare earth element in the fluorite block. In this case, it was supposed that the disordered potential, similar to the case of Zn doping in the CuO_2 plane, existed in the nonsuperconducting compound.[24] This might be a characteristic common to CuO_2 planes adjacent to a fluorite block.

The hole density in the Pb-32n2 phase with $n=3$, 5 slightly increased by cation substitution. However, it seems to be difficult for it to reach the optimal value for superconductivity, judging from the extrapolation of the measured data. The difficulty in optimal doping is also the reason for the absence of superconductivity in the Pb-32n2 phase with $n\geqslant 3$.

The sheet conductance per CuO_2 plane is similar for the Pb-3232 phase and Pb-3252 phase, as mentioned in Sec. III F. This means that the strength of localization does not increase when the distance between a pair of CuO_2 planes, d, increases from 0.87 nm to 1.44 nm. Then, the Pb-32n2 family with $n=3-8$ is useful in changing the c-axis transport while the in-plane transport is kept constant.

In the next phase of this study, our aim is to achieve control of the Josephson coupling along the c-axis using the Pb-32n2 family. To achieve this, it is desirable that the superconducting order parameter extend to the CuO_2 plane adjacent to the fluorite block in the Pb-32n2 phase. For cuprate superlattices, Bozovic and Eckstein already pointed out that hole depletion and localization in the interface CuO_2 plane are particularly important for the semiconducting or insulating spacer layer.[25] These two factors must be eliminated in order to obtain SIS tunnel junctions. In fact, their $(BiSrCa_3Cu_4O_x/3\times SrTiO_3/Cu_4Ca_3SrBiO_x)_n$ superlattice showed two-dimensional VRH.[25] In the present study, the CuO_2 plane in the Pb-3252 phase is doped with holes with nearly the same level as the superconductor, but the holes are weakly localized. The question is whether the proximity effect acts on the CuO_2 plane in a Pb-3252 unit cell inserted in a thick Pb-3212 superconductor, or not. Microscopic considerations are needed in order to answer this question but that information is not available now. So, we discuss the mesoscopic and macroscopic approaches based on the proximity effect in the conventional superconductor. Actually, the experimental results for the proximity effect (PE) in the high-

T_c $SN'S$ junctions, where N' is a cation-substituted superconductor with reduced T_c, are explained by the conventional PE theory.[26]

Recently, a theoretical study of the PE in a 2D disordered conductor, taking Coulomb interaction into account, has been reported.[27] This suggests that the PE appears in the disordered metal (resistivity ρ and thickness D) attached to a bulk superconductor except for the case of a sufficiently strong disorder. The critical value above which an energy gap due to PE in the normal metal vanishes is $t\lambda/4=1$, where $t=(e^2/2\pi^2\hbar)(\rho/D)$ expresses the strength of the disorder.[27] Here, λ is a dimensionless parameter concerning the Coulomb interaction and may be of the order of 0.1–1.[28] Substituting the sheet resistance per CuO_2 plane in the Pb-3252 sample (Fig. 11) into (ρ/D), we obtain $t=17.8$ at 30 K. Using this value, we are aware that our sample is near the border line. Unfortunately, the values of λ for the cuprates and our sample are as yet unknown and we cannot judge using the above criteria. In the layered cuprates, a CuO_2 plane with $p<0.05$ is an insulator. In this case, the conventional PE does not act effectively. Generally speaking, the coherence length in normal metal, ξ_N, increases with the carrier concentration. In a CuO_2 plane, however, excess holes with $p>0.3$ may be harmful to pair correlations. Therefore, we consider that $0.05<p<0.3$ is necessary for PE in the CuO_2 plane of the Pb-3252 phase. This condition has been satisfied in the present study. Thus, we may expect that the order parameter extends to the CuO_2 planes in the one-unit-cell-thick Pb-3252 phase inserted in the superconducting Pb-3212 layer. Such a layered structure can be constructed by using the MBE method, as shown in Fig. 3.

On the other hand, the recently constructed SO(5) theory of high-temperature superconductivity suggests that ξ_N in an underdoped nonsuperconducting cuprate is longer than the expected value from the conventional PE theory.[29] This means that superconducting order does not have to vanish on the atomic scale in the underdoped nonsuperconducting cuprate. This reinforces our argument in favor of the extension of the order parameter to the CuO_2 plane in the Pb-3252 phase.

V. SUMMARY

We have studied resistivity and thermopower for Pb-32n2 phase films with $n=1$, 3, and 5. This is a systematic study of the transport properties of separated pairs of pyramidal CuO_2 planes with $d>0.9$ nm. The growth conditions and compositions of the film samples were optimized to make conductive Pb-3252 films. We obtained the hole concentration $p=0.089$, which was within the range for the occurrence of superconductivity in layered cuprates, but resistivity still showed weak localization behavior. Here, the hole concentration p per [CuO] was estimated from the room-temperature thermopower. The electric conduction within a CuO_2 plane does not deteriorate with the increase of d from 0.87 nm (Pb-3232 phase) to 1.41 nm (Pb-3252 phase). Thus the Pb-32n2 phases with $n=3-8$ have the potential to control the Josephson coupling along the c axis.

For the Pb-3232 and Pb-3252 phases, the cation substitution of Ce^{4+} by Dy^{3+} makes resistivity and thermopower lower, but the increase in hole concentration is lower than expected from the simple calculation of the valence. The composition dependence of the c-axis length suggests that the cation deficiency exists in the multiple fluorite-type block layer. There are considered to be two reasons for the absence of superconductivity in the Pb-3232 and Pb-3252 phases. The first is that a disordered potential for charge carrier may exist in the CuO_2 planes. The cation deficiency in the fluorite block is a possible source of the disordered potential. The second reason is the difficulty in optimal doping.

ACKNOWLEDGMENTS

We would like to thank Dr. K. Ando, Dr. K. Sato, Dr. J. Yoshida, and Dr. N. Gemma of Toshiba Corporation for encouragement in this work and for illuminating discussion. We also thank M. Koike of Toshiba R&D Center for TEM observations and K. Kobayashi for providing the program to calculate XRD intensity. This study was supported by Special Coordination Funds for Promoting Science and Technology from the Japanese Science and Technology Agency, to which we are deeply indebted.

[1] R. Kleiner, F. Steinmeyer, G. Kunkel, and P. Müller, Phys. Rev. Lett. **68**, 2394 (1992); R. Kleiner and P. Müller, Phys. Rev. B **49**, 1327 (1994).

[2] J. Mannhart and H. Hilgenkamp, Supercond. Sci. Technol. **10**, 880 (1997).

[3] S. Ikegawa and Y. Motoi, Appl. Phys. Lett. **68**, 2430 (1996).

[4] S. Ikegawa and Y. Motoi, Physica C **282–287**, 673 (1997).

[5] S. L. Cooper and K. E. Gray, in *Physical Properties of High Temperature Superconductors IV*, edited by D. M. Ginsberg (World Scientific, Singapore, 1994), p. 61.

[6] S. Chakravarty, A. Sudbø, P. W. Anderson, and S. Strong, Science **261**, 337 (1993); S. Chakravarty and P. W. Anderson, Phys. Rev. Lett. **72**, 3859 (1994).

[7] P. W. Anderson, Science **268**, 1154 (1995).

[8] Z. Ye, H. Umezawa, and R. Teshima, Phys. Rev. B **44**, 351 (1991).

[9] S. Grabowski, J. Schmalian, M. Langer, and K. H. Bennemann, Phys. Rev. B **55**, 2784 (1997).

[10] H. Sawa, S. Suzuki, M. Watanabe, J. Akimitsu, H. Matsubara, H. Watabe, S. Uchida, K. Kokusho, H. Asano, F. Izumi, and E. Takayama-Muromachi, Nature (London) **337**, 347 (1989).

[11] Y. Tokura, T. Arima, H. Takagi, S. Uchida, T. Ishigaki, H. Asano, R. Beyers, A. I. Nazzal, P. Lacorre, and J. B. Torrance, Nature (London) **342**, 890 (1989).

[12] T. Wada, A. Ichinose, H. Yamauchi, and S. Tanaka, Physica C **171**, 344 (1990); T. Wada, K. Hamada, A. Ichinose, T. Kaneko, H. Yamauchi, and S. Tanaka, *ibid.* **175**, 529 (1991).

[13] T. Wada, A. Ichinose, F. Izumi, A. Nara, H. Yamauchi, H. Asano, and S. Tanaka, Physica C **179**, 455 (1991).

[14] A. Tokiwa, T. Oku, M. Nagoshi, and Y. Shono, Physica C **181**, 311 (1991).

[15] T. Wada, A. Nara, A. Ichinose, H. Yamauchi, and S. Tanaka, Physica C **192**, 181 (1992).

[16] C. Xianhui, D. Zhongfen, Q. Yitai, C. Zuyao, C. Zhaojia, and C.

Liezhao, Phys. Rev. B **48**, 9799 (1993).
[17] S. Ikegawa, Y. Motoi, and T. Miura, Physica C **229**, 280 (1994); Y. Motoi and S. Ikegawa, Appl. Phys. Lett. **73**, 987 (1998).
[18] S. Hosokawa and S. Ichimura, Rev. Sci. Instrum. **62**, 1614 (1991).
[19] S. D. Obertelli, J. R. Cooper, and J. L. Tallon, Phys. Rev. B **46**, 14928 (1992); J. L. Tallon, C. Bernhard, H. Shaked, R. L. Hitterman, and J. D. Jorgensen, *ibid.* **51**, 12911 (1995).
[20] R. J. Cava, M. Marezio, J. J. Krajewski, W. F. Peck, Jr., A. Santoro, and F. Beech, Physica C **157**, 272 (1989).
[21] T. Noji, T. Takabayashi, M. Kato, T. Nishizaki, N. Kobayashi, and Y. Koike, Physica C **255**, 10 (1995).
[22] Y. Koike, M. Masuzawa, T. Noji, H. Sunagawa, H. Kawabe, N. Kobayashi, and Y. Saito, Physica C **170**, 130 (1990).
[23] P. A. Lee and T. V. Ramakrishnan, Rev. Mod. Phys. **57**, 287 (1985).
[24] S. Ikegawa, T. Wada, T. Yamashita, H. Yamauchi, and S. Tanaka, Phys. Rev. B **45**, 5659 (1992).
[25] I. Bozovic and J. N. Eckstein, in *Physical Properties of High Temperature Superconductors V*, edited by D. M. Ginsberg (World Scientific, Singapore, 1996), p. 99.
[26] L. Antognazza, S. J. Berkowitz, T. H. Geballe, and K. Char, Phys. Rev. B **51**, 8560 (1995); L. Antognazza, B. H. Moeckly, T. H. Geballe, and K. Char, *ibid.* **52**, 4559 (1995).
[27] Y. Oreg, P. W. Brouwer, B. D. Simons, and A. Atland, Phys. Rev. Lett. **82**, 1269 (1999).
[28] A. M. Finkel'stein, Z. Phys. B: Condens. Matter **56**, 189 (1984).
[29] E. Delmer, A. J. Berlinsky, C. Kalin, G. B. Arnold, and M. R. Beasley, Phys. Rev. Lett. **80**, 2917 (1998).